Korteweg–De Vries–Burger Equation with Jeffreys' Wind–Wave Interaction: Blow-Up and Breaking of Soliton-like Solutions in Finite Time

Miguel Alberto Manna, Anouchah Latifi

fluids

MDPI

Article

Korteweg–De Vries–Burger Equation with Jeffreys' Wind–Wave Interaction: Blow-Up and Breaking of Soliton-like Solutions in Finite Time

Miguel Alberto Manna [1] and Anouchah Latifi [2,*]

[1] Laboratoire Charles Coulomb-UMR 5221 CNRS, Université de Montpellier, F-34095 Montpellier, France; miguel.manna@umontpellier.fr
[2] Departement of Mechanics, Qom University of Technology, Qom 1519-37195, Iran
* Correspondence: latifi@qut.ac.ir

Abstract: In this study, the evolution of surface water solitary waves under the action of Jeffreys' wind–wave amplification mechanism in shallow water is analytically investigated. The analytic approach is essential for numerical investigations due to the scale of energy dissipation near coasts. Although many works have been conducted based on the Jeffreys' approach, only some studies have been carried out on finite depth. We show that nonlinearity, dispersion, and anti-dissipation are the dominating phenomena, obeying an anti-diffusive and fully nonlinear Serre–Green–Naghdi (SGN) equation. Applying an appropriate perturbation method, the current research yields a Korteweg–de Vries–Burger-type equation (KdV-B), combining weak nonlinearity, dispersion, and anti-dissipation. This derivation is novel. We show that the continuous transfer of energy from wind to water results in the growth over time of the KdV-B soliton's amplitude, velocity, acceleration, and energy, while its effective wavelength decreases. This phenomenon differs from the classical results of Jeffreys' approach and is due to finite depth. In this study, it is shown that expansion and breaking occur in finite time. These times are calculated and expressed with respect to soliton- and wind-appropriate parameters and values. The obtained values are measurable in experimental facilities. A detailed analysis of the breaking time is conducted with regard to various criteria. By comparing these times to the experimental results, the validity of these criteria are examined.

Keywords: wind-generated waves; wind-wave growth rates; Jeffreys' theory; finite depth; korteweg-de vries-burger equation

Citation: Manna, M.A.; Latifi, A. Korteweg–De Vries–Burger Equation with Jeffreys' Wind–Wave Interaction: Blow-Up and Breaking of Soliton-like Solutions in Finite Time. *Fluids* **2023**, *8*, 231. https://doi.org/10.3390/fluids8080231

Academic Editor: D. Andrew S. Rees

Received: 20 June 2023
Revised: 7 August 2023
Accepted: 17 August 2023
Published: 19 August 2023

1. Introduction

Theoretical studies on the growth rate of linear surface wind–waves in deep or finite water depths constitute a significant matter of investigation in fluid dynamics (see, for instance, Li and Shen [1] and Bonfils et al. [2]). Surface wind–wave growth theories in deep water have been initiated by the pioneering works of Jeffreys [3,4], Phillips [5], and Miles [6]. Thomas et al. [7] and Montalvo et al. [8,9] have extended the Miles theory to finite depth. More recent studies on finite depth were conducted by Kadam et al. [10].

In Jeffreys' and Miles' approaches, water is considered deep and irrotational, and the water and air dynamic equations are linearized. Consequently, the wave amplitude $\eta(x,t,k)$, where x is the spatial coordinate, t is time, and k is the wave number, grows exponentially over time, more or less quickly, according to the value of the wave growth rate β. Namely, $\eta(x,t,k) \sim \exp \beta t$.

Moreover, Jeffreys' and Miles' theories were limited to the deep-water domains. For the first time, Montalvo et al. [8,9] have highlighted the important role that finite depth plays from a theoretical point of view. The principal purpose of these studies was to provide solid physical–mathematical models with which to understand coastal processes of wind–wave generation. The models proposed in these studies are in fair agreement with

the data and empirical relationships obtained from the Lake George experiment as well as with the data from the Australian Shallow Water Experiment (Donelan et al. [11,12], Young [13,14]). Recently, in experimental facilities, Branger et al. [15] studied the effect of finite depth on wave growth. The results obtained from these studies were in agreement with the theoretical curves predicted by Montalvo et al. [8].

Beyond the linear and dispersionless approximations made in references [3] to [15], specific phenomena are due to nonlinearity and dispersion. Nonlinearity implies that both wave phase velocity and wavelength depend on wave amplitude, and dispersion implies that the group velocity depends on the wave number (Whitham [16]).

This paper aims to study the simultaneous influence of nonlinearity, dispersion, and wind anti-dissipative forcing on wave dynamics. More specifically, our study concerns weak nonlinearity and dispersion under wind action. In this approach, the wave dynamics are described using the soliton solution of a KdV-B-type equation (Benney [17], Johnson [18], Grad and Hu [19], Hu [20], Wadati [21], Karahara [22]) with anti-dissipation. The weakly nonlinear and anti-dispersive KdV-B type equation is derived from a *fully nonlinear Serre–Green–Nagdhi system* (Serre [23], Green et al. [24], Green and Naghdi [25], Su and Gardner [26]) using a reformulated Whitham's method [16]. In recent years, various novel analytical techniques have been developed to solve nonlinear equations and find a diversity of solitary wave solutions (see, for instance, Shah et al. [27,28], Zhang et al. [29], and Shakeel et al. [30]).

The paper is organized as follows: In Section 2.1, dimensionless Serre–Green–Naghdi (SGN) equations considering wind action with Jeffrey's mechanism are presented. In Section 2.2, applying an appropriate perturbative method, the Korteweg–de Vries–Burger equation is derived from SGN equations. In Section 2.3, a soliton-like solution of the KdV-B equation is given. Section 2.4 shows that the soliton solution of the KdV-B equation has a decreasing effective wavelength and a growing amplitude over time and blows up within a *finite time* while keeping its symmetric shape. Therefore, it is clear that the wave breaking that occurs before the blow-up must have other physical reasons. In Section 3, we apply various wave-breaking criteria to the KdV-B solution and find the breaking time and various characteristics of the wave at the breaking time in each case. Section 4 presents calculations of the breaking time for specific values of depth and wind speed at a height of 10 m. Finally, in Section 5, conclusions are drawn and discussed.

2. Materials and Methods

2.1. Dimensionless Green–Naghdi Equations

Green–Naghdi equations under wind action (Green et al. [24], Green and Naghdi [25], Manna et al. [31]) are as follows:

$$u_t + uu_x + g\eta_x = -\frac{1}{\rho_w}[P_a(x,\eta,t]_x + \frac{1}{3(\eta+h)}\{(\eta+h)^3(u_{xt} + uu_{xx} - u_x^2)\}_x, \tag{1a}$$

$$\eta_t + [u(\eta+h)]_x = 0, \tag{1b}$$

where $u(x,z,t)$ is a fluid's horizontal velocity, which we assume to be independent of z, i.e., $u(x,z,t) = u(x,t)$; $P_a(x,z,t)$ is the Archimedean air pressure taken at the perturbed water surface $z = \eta(x,t)$; $\eta(x,t)$ is wave amplitude; g is gravitational acceleration; ρ_w is water density; and h is water depth. Subscripts x and t denote partial derivatives with respect to x and t, respectively.

If $P_a = P_0 =$ constant, Equations (1a)–(1b) reduce to the usual Green–Naghdi equations. The Jeffreys' sheltering mechanism assumes that $P_a = P_a(x,z,t)$. The air pressure on the windward wave's face is larger than the seaward wave's face, which causes a continuous energy transfer from the wind to the wave.

Jeffreys [3,4] showed that the pressure $P_a(x,z,t)$ evaluated on the surface, i.e., $P_a = P_a(x,z=\eta,t)$, can be expressed as follows:

$$P_a(x,z=\eta,t) = \rho_a \epsilon (U_{10} - c)^2 \eta_x(x,t), \tag{2}$$

where ϵ is the *sheltering coefficient*, ρ_a is the air density, U_{10} is the wind velocity at a height of 10 m, and $c = (g/k)^{1/2} \tanh^{1/2}(kh)$. Substituting Equation (2) into Equations (1a) and (1b) yields

$$u_t + uu_x + g\eta_x = -\epsilon s\Delta^2 \eta_{xx} + \frac{1}{3(\eta+h)}\{(\eta+h)^3(u_{xt} + uu_{xx} - u_x^2)\}_x, \tag{3a}$$

$$\eta_t + [u(\eta+h)]_x = 0, \tag{3b}$$

where $s = \frac{\rho_a}{\rho_w} \sim 10^{-3}$ and $\Delta = U_{10} - c$.

We introduce dimensionless "primed" variables, x', t' and η', as follows:

$$x = \lambda_0 x', \qquad t = \frac{\lambda_0}{c_0} t', \qquad \eta = a_0 \eta', \tag{4}$$

where $c_0 = (gh)^{1/2}$, a_0 and λ_0 are initial typical wave amplitude and wavelength, respectively. In addition, we define two fundamental parameters commonly used in classical water surface studies, namely, ν and δ, as follows:

$$\nu = \frac{a_0}{h}, \qquad \delta = \frac{h}{\lambda_0}. \tag{5}$$

Finally, in order to obtain the dimensionless, scaled Green–Naghdi equations of motion, the following scaling is required (Johnson [18]):

$$u = \nu u_0. \tag{6}$$

By introducing Equations (4)–(6) into Equations (3a) and (3b), we obtain the following dimensionless equations

$$u_{0,t} + \nu u_0 u_{0,x} + \eta_x = -\epsilon s\Delta^2 \delta \eta_{xx} + \frac{\delta^2}{3(1+\nu\eta)}\{(1+\nu\eta)^3(u_{0,xt} + \nu u_0 u_{0,xx} - \nu u_{0,x}^2)\}_x, \tag{7a}$$

$$\eta_t + [u_0(1+\nu\eta)]_x = 0, \tag{7b}$$

where, for convenience, the "primes" of dimensionless quantities are omitted.

2.2. Korteweg–De Vries–Burger Equation

In this section, we derive the KdV-B equations from SGN Equations (7a) and (7b). To this aim, we consider a wave moving from left to right (Whitham [16]). At the lowest order, by neglecting the terms of order ν and δ and any higher orders, Equations (7a) and (7b) are reduced to

$$u_t + \eta_x = 0, \tag{8a}$$

$$\eta_t + u_x = 0. \tag{8b}$$

Equations (8a) and (8b) are equivalent to

$$\eta_{tt} + \eta_{xx} = 0, \qquad \text{or} \qquad u_{tt} + u_{xx} = 0, \tag{9}$$

and

$$u_x(x,t) = \eta(x,t), \tag{10}$$

is a solution of Equations (8a) and (8b).

Now, we look for a perturbed solution with the following form (Whitham [16]):

$$u = \eta + \nu\mathbb{A} + \delta\mathbb{B} + \delta^2\mathbb{C} + O(\delta\nu, \delta^2\nu, \nu^2), \tag{11}$$

where $\mathbb{A}$, $\mathbb{B}$, and $\mathbb{C}$ are functions of η and its derivatives. By inserting Equation (11) into Equations (7a) and (7b), we obtain

$$\eta_t + \eta_x + \nu(\mathbb{A}_t + \eta\eta_x) + \delta(\mathbb{B}_t + \epsilon s\Delta^2\eta_{xx}) + \delta^2(\mathbb{C}_t - \frac{1}{3}\eta_{xxt}) + O(\delta\nu, \delta^2\nu, \nu^2) = 0, \quad (12a)$$

$$\eta_t + \eta_x + \nu(\mathbb{A}_x + \eta\eta_x) + \delta(\mathbb{B}_x + \delta^2\mathbb{C}_x + O(\delta\nu, \delta^2\nu, \nu^2) = 0, \quad (12b)$$

where

$$\eta_t = -\eta_x + O(\delta\nu, \delta^2\nu, \nu^2). \quad (13)$$

Therefore, in Equation (12a), all the t-derivatives may be substituted by $-\partial_x$. Hence, Equations (12a) and (12b) are compatible if

$$\mathbb{A} = -\frac{1}{4}\eta^2, \qquad \mathbb{B} = \frac{1}{2}s\epsilon\Delta^2\eta_x, \qquad \mathbb{C} = \frac{1}{6}\eta_{xx}. \quad (14)$$

Substituting Equation (14) into Equations (12a) and (12b) yields

$$\eta_t + \eta_x + \frac{3}{2}\nu\eta\eta_x + \frac{\delta^2}{6}\eta_{xxx} + s\epsilon\frac{\delta}{2}\Delta^2\eta_{xx} = 0, \quad (15a)$$

$$u - \eta + \frac{\nu}{4}\eta^2 - s\epsilon\frac{\delta}{2}\Delta^2\eta_x - \frac{1}{6}\delta^2\eta_{xx} = 0. \quad (15b)$$

Equation (15a) is the KdV-B equation appearing in various physical contexts such as wave–particle interactions, dust charge fluctuations in dusty plasma, multi-ion streaming, Landau damping, etc. (f.i., see Adriani et al. [32] and Cheng et al. [33]), while Equation (15b) is a Riemann invariant.

Notice that an analogous study was carried out by Manna et al. [34], starting from a weak nonlinear Boussinesq equation.

2.3. Solution of Korteweg–De Vries–Burger Equation

In order to find the solution of Equation (15a), we apply the following change of variables:

$$\sigma = x - t, \qquad t_1 = \delta^2 t. \quad (16)$$

Hence, Equation(15a) becomes

$$\eta_{t_1} + \frac{3}{2}\eta\eta_\sigma + \frac{\delta^2}{6\nu}\Delta^2\eta_{\sigma\sigma\sigma} + \frac{\delta}{2\nu}\Delta^2 s\eta_{\sigma\sigma} = 0. \quad (17)$$

It is worth noticing that the limit of Equation (17), as $s \to 0$ yields to the well known KdV equation:

$$\eta_{t_1} + \frac{3}{2}\eta\eta_\sigma + \frac{\delta^2}{6\nu}\Delta^2\eta_{\sigma\sigma\sigma} = 0. \quad (18)$$

This result is quite natural since $s \to 0$ amounts to neglecting the action of the wind. Therefore, it is possible to assume that the KdV-B solution, Equation (17), has the same form as the solution of Equation (18), namely

$$\eta(\sigma, t_1) = \frac{a}{\cosh^2[P(\sigma - c't_1)]}. \quad (19)$$

This is the typical soliton solution of the KdV equation, with one difference, however: the amplitude a in Equation (19) can be time-dependant, whereas the amplitude of KdV equation is not.

By inserting Equation (19) into Equation (17), we obtain

$$P = \sqrt{\frac{3\nu}{4\delta^2}}, \qquad c' = \frac{a}{2}. \quad (20)$$

Now, the task is to find the time-dependent expression of $a(t)$ in Equation (19). Noticing that the anti-diffusive term $\frac{\delta}{2\nu}\Delta^2 s\eta_{\sigma\sigma}$ in Equation (17) is of the order δ^3 and small enough at $t = 0$, one can find the solution of Equation (17) via perturbation. For this purpose, we introduce a slow time t_2, as follows

$$t_2 = \delta^2 t_1 = \delta^3 t, \tag{21}$$

and we expand η in terms of δ, as follows

$$\eta = \eta_0(\sigma, t_2) + \delta\eta_1(\sigma, t_2) + O(\delta^2), \tag{22}$$

where η_0 is the solution given by Equation (19).

By introducing ν_0 in the following manner

$$\nu = \nu_0\delta^2, \tag{23}$$

and inserting Equation (22) into Equation (17), we obtain

at order 0 of δ

$$\frac{\partial\eta_0}{\partial t_1} + \frac{3}{4}\nu_0\eta_0\frac{\partial\eta_0}{\partial\sigma} + \frac{1}{6}\frac{\partial^3\eta_0}{\partial\sigma^3} = 0, \tag{24a}$$

and *at order 1 of* δ*:*

$$\frac{\partial\eta_1}{\partial t_1} + \frac{3}{2}\nu_0\eta_0\frac{\partial\eta_1}{\partial\sigma} + \frac{3}{2}\nu_0\eta_{0,\sigma}\eta_1 + \frac{1}{4}\nu_0\frac{\partial^3\eta_1}{\partial\sigma^3} = -\eta_{0,t_2} - \frac{s_0}{2}\epsilon\Delta_0^2\eta_{0,\sigma\sigma}. \tag{24b}$$

By introducing operators $\widehat{L}_0$ and $\widehat{L}_1$ as follows

$$\widehat{L}_0 = \frac{\partial}{\partial t_1} + \frac{3}{4}\nu_0\eta_0\frac{\partial}{\partial\sigma} + \frac{1}{6}\frac{\partial^3}{\partial\sigma^3}, \tag{25a}$$

$$\widehat{L}_1 = \frac{\partial}{\partial t_1} + \frac{3}{2}\nu_0\left(\eta_0\frac{\partial}{\partial\sigma} + \eta_{0,\sigma}\right) + \frac{1}{4}\nu_0\frac{\partial^3}{\partial\sigma^3}. \tag{25b}$$

Equations (25a) and (25b) read

$$\widehat{L}_0\eta_0 = 0, \tag{26a}$$

$$\widehat{L}_1\eta_1 = -\eta_{0,t_2} - \frac{s_0}{2}\epsilon\Delta_0^2\eta_{0,\sigma\sigma}. \tag{26b}$$

For further progress, we apply Green's theorem in one dimension. One can find the application of this theorem to linear differential operators in various works (Dunkel [35], Svendsen [36], Chiang [37]). In particular, the damping of solitary waves [38,39] has been shown using this theorem, and an extension to matrix differential operators has been carried out by Manna and Latifi [40]. Green's theorem in one dimension (Darboux [41]) provides us with

$$\int_a^b [zP(y) - y\bar{P}(z)]dx = [P(y,z)]_a^b, \tag{27}$$

where P is a linear differential operator and y and z any two functions of x and $\bar{P}(z)$ and $P(y,z)$ are the adjoint and the bilinear differential expressions of $P(y)$, respectively.

Applying Green's theorem to our case by replacing Equations (25a) and (25b) in Equation (27) yields

$$\int_{-\infty}^{+\infty}\left(\eta_0\widehat{L}_1\eta_1 - \eta_1\widehat{L}_0\eta_0\right)d\sigma = 0. \tag{28}$$

Notice that the right-hand side of (28) is null due to the symmetric behavior of η_0 and η_1 at $\pm\infty$. By replacing η_0 from Equation (19) with a time-dependent amplitude $a(t_2)$, Equation (28) yields the following:

$$a(t_2) = \frac{1}{1 - \frac{2}{5}\frac{s\epsilon\Delta^2}{\delta^2}t_2}. \tag{29}$$

Using the approximation $O(\nu) = O(\delta^2)$, Equation (21) can equivalently be written as $t_2 = \nu\delta t$. Hence, Equation (29) becomes

$$a(t) = \frac{1}{1 - \frac{t}{t_b}}, \tag{30}$$

where

$$t_b = \frac{5\delta}{2\epsilon s\Delta^2\nu}. \tag{31}$$

In Equation (30), it can be seen that the amplitude $a(t) \to \infty$ when $t \to t_b$, which we call the blow-up time. Hence, the solution of (15a) is as follows:

$$\eta = a(t)\cosh^{-2}(\theta), \tag{32}$$

where

$$\theta(x,t) = \alpha a^{1/2}\left[x - t + \frac{\nu}{2}t_b\ln\left(1 - \frac{t}{t_b}\right)\right], \qquad \alpha = \left(\frac{3}{4}\frac{a_0}{h}\right)^{1/2}\frac{\lambda_0}{h}, \tag{33}$$

2.4. Blow-Up in Finite Time and the Evolution of the Soltion's Shape

In this section, we shall study the evolution of the soliton's shape over time, i.e., Equation (32), before the blow-up time t_b.

Returning to variables with dimensions, Equation (4), that is, the solution of KdV-B, i.e., Equation (32), is expressed as follows:

$$\eta(x,t) = \frac{a_0}{1 - \frac{t}{t_b}}\cosh^{-2}\left\{\frac{\alpha}{(1 - \frac{t}{t_b})^{1/2}}\frac{1}{\lambda_0}\left[x - c_0 t + \frac{\nu}{2}c_0 t_b\ln\left(1 - \frac{t}{t_b}\right)\right]\right\}. \tag{34}$$

For $t = 0$, we have

$$\eta(x,0) = a_0\cosh^{-2}\left(\frac{\alpha}{\lambda_0}x\right), \tag{35}$$

where

$$\alpha^2 = \frac{3\nu}{4\delta^2} = \frac{3}{4}\frac{a_0{\lambda_0}^2}{h^3}. \tag{36}$$

Using Equation (36), the blow-up time, t_b, can also be expressed as follows for further use:

$$t_b = \frac{5}{2}\frac{c_0 h^2}{\epsilon s a_0\Delta^2}. \tag{37}$$

The wave number k and the frequency ω, for a monochromatic progressive wave with a phase $\theta(x,t) = kx - \omega t$, are defined as follows:

$$k = \frac{\partial\theta}{\partial x}, \qquad \omega = -\frac{\partial\theta}{\partial t}. \tag{38}$$

These definitions can be generalized for k and ω depending on x and t:

$$k(x,t) = \frac{\partial\theta}{\partial x}(x,t), \qquad \omega(x,t) = -\frac{\partial\theta}{\partial t}(x,t). \tag{39}$$

By employing Equations (30), (33), and (39), the wavelength $\lambda(t)$ and the wave number $k(t)$ of the soliton solution (32) can be defined as follows:

$$\lambda(t) = \frac{\lambda_0}{\alpha}\left(1 - \frac{t}{t_b}\right) = \left(\frac{4h}{3a_0}\right)^{1/2} h\left(1 - \frac{t}{t_b}\right)^{1/2}, \tag{40}$$

$$k(t) = \left(\frac{3a_0}{4h}\right)^{1/2} \frac{1}{h}\left(1 - \frac{t}{t_b}\right)^{-1/2} = \alpha a^{1/2}(t). \tag{41}$$

We define the effective wave number, denoted as $\widetilde{k}$, as follows:

$$\widetilde{k} = \frac{\alpha}{\lambda_0} = \left(\frac{3a_0}{4h}\right)^{1/2} \frac{1}{h}, \tag{42}$$

and we define the associated effective wavelength, denoted as $\widetilde{\lambda}$, as follows:

$$\widetilde{\lambda} = \frac{1}{\widetilde{k}} = \left(\frac{4h}{3a_0}\right)^{1/2} h. \tag{43}$$

It is worth noting that for $t \to t_b$, Equations (40), (41), and (30) yield

$$\lim_{t \to t_b} \lambda(t) = 0, \qquad \lim_{t \to t_b} k(t) = \infty, \qquad \lim_{t \to t_b} a(t) = \infty, \tag{44}$$

respectively. This is the first indication of the narrowing of the soliton's shape while its amplitude $a(t)$ grows.

For further exploration, we examine the speed of the phase planes on either side of the soliton's crest. Using Equation (41), it is useful to write Equation (33) as a function of $k(t)$, as follows

$$\theta(x,t) = k(t)(x - t) + \nu t_b k(t)[\ln(x) - \ln(k(t))]. \tag{45}$$

Using Equation (41), we obtain

$$\frac{\partial k(t)}{\partial t} = \frac{k^3(t)}{2\alpha^2 t_b}. \tag{46}$$

Employing Equations (39) and (46) together yields ω as a function of $k(t)$:

$$\omega(x,t) = -\frac{k^3(t)}{2\alpha^2 t_b}(x - t) + k(t) - \nu t_b \frac{k^3(t)}{2\alpha^2 t_b}\left[\ln\left(\frac{\alpha}{k(t)} - 1\right)\right]. \tag{47}$$

The dimensionless phase velocity $c(x,t)$ of the soliton solution is

$$c(x,t) = \frac{\omega(x,t)}{k(t)} = 1 + \frac{\nu}{2\alpha^2}k^2(t) - \frac{k(t)\theta(x,t)}{2\alpha^2 t_b}, \tag{48}$$

which, by using Equation (41), can be equivalently written as a function of $a(t)$, as follows

$$c(x,t) = 1 + \frac{\nu}{2}a(t) - \frac{a^{1/2}(t)}{2\alpha t_b}\theta(x,t). \tag{49}$$

The position of the soliton's crest can be found by solving

$$\theta(x,t) = 0, \tag{50}$$

at any time t. The dimensionless phase θ is provided by the first of the equations in Equation (33), while the phase velocity c is given by Equation (49). Therefore, the position of the soliton's crest and the velocity of the soliton at its crest are

$$x_{crest}(t) = t + \frac{\nu t_b}{2} \ln[a(t)], \tag{51}$$

$$c(x_{crest}, t) = 1 + \frac{\nu}{2} a(t), \tag{52}$$

respectively.

By incorporating Equations (49) and (33), the phase speed becomes

$$\begin{aligned} c &= c_{crest} - \frac{\alpha}{2} \frac{a(t)}{t_b} \left[(x - t) - \frac{\nu}{2} t_b \ln[a(t)] \right] \\ &= c_{crest} - \frac{\alpha}{2} \frac{a(t)}{t_b} [x - x_{crest}]. \end{aligned} \tag{53}$$

Therefore, the speeds of the phase planes at $(x_{crest} - \Delta x)$ and $(x_{crest} + \Delta x)$ are

$$c_{crest-\Delta x} = c_{crest} + \frac{\alpha}{2} \frac{a(t)}{t_b} \Delta x, \tag{54a}$$

$$c_{crest+\Delta x} = c_{crest} - \frac{\alpha}{2} \frac{a(t)}{t_b} \Delta x, \tag{54b}$$

respectively. Hence,

$$c_{crest-\Delta x} > c_{crest} > c_{crest+\Delta x}. \tag{55}$$

This means that the phase planes on the left side of x_{crest} have a greater speed than the phase planes on the right side of x_{crest}, resulting in a narrowing of the soliton's shape while its amplitude $a(t)$ grows (Figure 1).

Moreover, there is no symmetry breaking in the soliton's shape since, according to Equations (54a) and (54b), the symmetric phase planes on either side of x_{crest} have equal speeds when moving toward the phase plane at x_{crest}, namely, $\frac{\alpha}{2} \frac{a(t)}{t_b} \Delta x$. This speed grows over time with the amplitude $a(t)$. Therefore, wave breaking does not result directly from the soliton solution of the KdV-B equation. Hence, one should consider other criteria to explain wind–wave breaking before the blow-up time. These criteria shall be considered in the next section.

It should also be noticed that the propagation speed of the soliton is the speed of its crest, namely, c_{crest}.

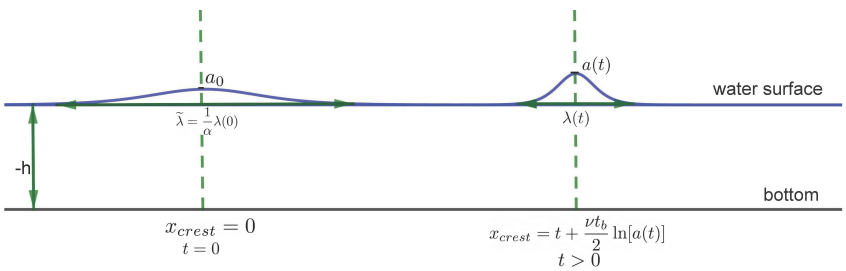

Figure 1. On the left, the soliton is plotted at $t = 0$. The amplitude at crest is a_0, and its effective wavelength is $\widetilde{\lambda}$. The origins of the coordinates are placed at their crest positions. On the left side, at $t > 0$, the soliton has moved to the right, its shape has sharpened ($\lambda(t) < \widetilde{\lambda}$), and its amplitude has grown ($a(t) > a_0$). For convenience, scales are not respected.

3. Wave-Breaking Criteria

As noted in the previous section, wave breaking does not result from the evolution of the wave as the soliton solution of the KdV-B equation. Therefore, we must consider other reasons for wave breaking. The most well-known criteria of wave breaking for linear monochromatic waves are the McCowan criterion [42], the Miche criterion [43], and the horizontal velocity criterion (Shemer [44]). However, as we shall see, these latest criteria cannot be applied to our case. Therefore, we propose an alternative criterion that we shall call the "alternative velocity criterion". For further use, we denote $t_{d,Mc}$, $t_{d,Mi}$, and $t_{d,alv}$ as the wave-breaking times within the McCowan criterion, the Miche criterion, and the alternative velocity criterion, respectively.

In what follows, we will compute the breaking time t_d, as well as the amplitude, the wavelength, and the phase velocity, of a solitary wave at $t = t_d$ within each of the mentioned criteria.

3.1. McCowan Criterion

The McCowan criterion is established for linear solitary waves and concerns the maximum height that such waves might attain without breaking. McCowan has shown that breaking occurs at a given rate between the maximum wave amplitude a_{max} and the water depth h, namely

$$\frac{a_{max}}{h} \approx 0.78. \tag{56}$$

Applying this criterion to the soliton solution Equation (34), where $a(t) = a_0(1 - \frac{t}{t_b})^{-1}$, Equation (56) yields

$$\left(\frac{a_0}{h}\right)\frac{1}{1 - \frac{t_{d,Mc}}{t_b}} \approx 0.78. \tag{57}$$

Equation (57) gives the breaking time according to McCowan criterion, which is

$$t_{d,Mc} \approx t_b(1 - 1.28\nu). \tag{58}$$

Using Equation (34), it is easy to calculate the maximum height reached at $t = t_{d,Mc}$:

$$\eta_{max} = a_{max} \approx \frac{a_0}{1.28\nu} \approx 0.78h. \tag{59}$$

In addition, by employing Equation (40), one obtains the soliton's wavelength at the moment of wave breaking, namely, $\lambda(t_{d,Mc})$:

$$\lambda(t_{d,Mc}) \approx 1.28\left(\frac{4}{3}a_0 h\right)^{1/2}. \tag{60}$$

3.2. Miche Criterion

The Miche criterion is based on empirical observations of linear waves' dispersion relations at a finite depth h with a wave length of λ. The Miche criterion fixes the maximum height a_{max} reached by a wave before it breaks, as follows

$$\left(\frac{a}{\lambda}\right)_{max} = \frac{1}{7}\tanh\left(\frac{2\pi h}{\lambda}\right). \tag{61}$$

In our case, by replacing a with $a(t) = a_0(1 - \frac{t}{t_b})^{-1}$ and λ with Equation (40), on the right side of Equation (61), we obtain

$$\left(\frac{a}{\lambda}\right)_{max} = \frac{\nu}{2}(3\nu)^{1/2}\left(1 - \frac{t_{d,Mi}}{t_b}\right)^{3/2}. \tag{62}$$

Now, by replacing λ with Equation (40) on the left side of Equation (61), employing $\nu = a_0/h$, assuming $t = t_{d,Mi}$, and expanding the hyperbolic tangent of $\left(\frac{a}{\lambda}\right)_{max}$ up to the order $(3\nu)^{3/2}$, we obtain

$$\frac{1}{7}\tanh\left(\frac{2\pi h}{\lambda}\right) = \frac{1}{7}\frac{\pi(3\nu)^{1/2}}{(1-\frac{t_{d,Mi}}{t_b})^{1/2}} - \frac{1}{21}\frac{\pi^3(3\nu)^{3/2}}{(1-\frac{t_{d,Mi}}{t_b})^{3/2}} + O(\nu^{5/2}). \tag{63}$$

Using Equations (61)–(63) and neglecting terms of a higher order than ν, we obtain

$$t_{d,Mi} = t_b\left(1 - \frac{7\nu}{2\pi} - \pi^2\nu\right). \tag{64}$$

The maximum height reached by the wave at $t = t_{d,Mi}$ is

$$\eta_{max} = a_{max} \approx \frac{0.09a_0}{\nu} \approx 0.09h. \tag{65}$$

Using Equations (62) and (64), the soliton's wavelength can be calculated at $t = t_{d,Mi}$:

$$\lambda_{max} \approx 4.7 \times 10^{-3}\left(\frac{h}{a_0}\right)^{5/2} h. \tag{66}$$

3.3. Alternative Horizontal Velocity Criterion

The horizontal velocity criterion assumes that wave breaking occurs when the group velocity of a water plane wave exceeds the speed of the phase plane at the crest. In our case, this criterion cannot be applied because, at the first approach, the group velocity does not have a significant impact on a solitary wave. Therefore, we replace this criterion with an alternative approach, assuming that wave breaking occurs when the fluid horizontal velocity exceeds the phase plane velocity at the crest. At this moment, matter starts to be ejected from a wave.

The phase plane velocity is expressed as shown in Equation (49). The phase velocity at the crest, i.e., for $\theta(x,t) = 0$, is given in Equation (52). The horizontal water velocity is given in Equation (15b). Using Equations (6) and (22), as well as (21) or, equivalently, $t_2 = \nu\delta t$, the water velocity can be expanded as follows

$$u_0 = \eta - \frac{\nu}{4}\eta^2 + O(\delta, \delta^2). \tag{67}$$

It can be seen from Equation (32) that at the crest, $\eta(\theta = 0) = a(t)$. Hence, the alternative velocity criterion is as follows:

$$1 + \frac{\nu}{2}a \geq a - \frac{\nu}{4}a^2 \tag{68}$$

The above inequality yields the following quadratic equation

$$a^2 + \left(2 - \frac{4}{\nu}\right)a + \frac{4}{\nu} \geq 0 \tag{69}$$

Considering the fact that ν is a small parameter, the solution of Equation (69) is $a \lessapprox \frac{1}{2}$ and $a \gtrapprox \frac{4}{\nu} - \frac{5}{2}$. The first part of the solution is not acceptable since it corresponds to negative times, while the latter, using Equation (30) and neglecting the terms of order ν^2, yields the breaking time $t_{d,alv}$, as follows

$$t_{d,alv} \approx t_b\left(1 - \frac{\nu}{4}\right). \tag{70}$$

By incorporating Equation (34), the maximum height reached at $t = t_{d,alv}$ is expressed as

$$a_{max}(t_{d,alv}) \approx 4h. \tag{71}$$

The wave length at $t = t_{d,a}$ is obtained from Equation (40), and it is expressed as follows:

$$\lambda(t = t_{d,alv}) = \left(\frac{1}{3}\right)^{1/2} h. \tag{72}$$

4. Results

In order to calculate the specific values of breaking time, wave amplitude, wave length, wave speed, and the distance traveled by a solitary wave at the breaking time in accordance with each of the criteria studied in the previous section, we must calculate the blow-up time for different values of depth and wind speed at a height of 10 meters. This calculation can be performed using Equation (37). Specific values of the breaking time t_d are shown in (Table 1) for a depth ranging from 20 cm to 100 cm, covering shallow and intermediate water depths (Young [14]), and a wind speed at 10 m, denoted as U_{10}, ranging from 10 m/s to 30 m/s.

Table 1. In this table, blow-up times t_b (s) are calculated for different values of depth h (cm) and wind speed at 10 m height U_{10} (m/s).

U_{10} \ h	**20**	**30**	**40**	**50**	**60**	**70**	**80**	**90**	**100**
10	247	556	998	1543	2222	3025	3951	5000	6173
15	102	230	408	638	918	1250	1633	2066	2551
20	55	125	222	346	499	679	886	1122	1385
30	24	54	95	149	214	291	381	482	595

Using the values in Table 1, it is easy to calculate the breaking time t_d and various characteristics of a wave at t_d. In (Table 2), we chose a typical wind speed at 10 m $U_{10} = 15$ m/s and a typical depth $h = 60$ cm. Using Equations (58) and (59), we calculated $t_{d,Mc}$ and a_{max} for the McCowan criterion; we derived Equations (64) and (65), yielding $t_{d,Mi}$, and a_{max} for the Miche criterion; and, finally, we derived Equations (70) and (71), yielding $t_{d,Mi}$, and a_{max} for the alternative velocity criterion.

Table 2. The breaking time t_d and the maximum height a_{max} reached by the soliton before breaking were calculated in accordance with the McCowan, Miche, and alternative velocity criteria for $U_{10} = 15$ m/s and $h = 60$ cm, representing a typical wind speed at 10 m and a typical depth, respectively.

Criterion	**McCowan**	**Miche**	**Alternative Velocity**
t_d	879	582	910
a_{max}	47	5	240

5. Conclusions

In the context of wind–wave interaction under the action of Jeffrey's mechanism, using the SGN equation as a basis, we derived—through an appropriate perturbation method—the KdV-B equation. To our knowledge, this derivation method is novel.

The soliton-like solution of the KdV-B equation was analytically obtained, and it was shown that the wavelength of this solitary wave decreases in time while its amplitude grows and *expands in finite time*. The blow-up time was analytically calculated, and its numerical values were obtained for various wind speeds at 10 m and for various depths.

The evolution over time of the soliton solution's shape was rigorously studied, and it was proved that the symmetry of this soliton never breaks. Therefore, one must consider other physical reasons for a wave breaking before a blow-up. For this reason, we calculated

the breaking time for the most well-known criteria, namely, the McCowan and Miche criteria. We also pointed out that a third well-known criterion for wave breaking, namely, "the velocity criterion", cannot be applied in the case of solitary waves. Hence, we have proposed an alternative to the latter criterion.

The values we have obtained are all measurable in experimental facilities and in situ. Indeed, the range of wind speeds at 10 m, as well as the rage of depths, are typical values. Moreover, the breaking times and the maximum amplitudes reached by the wave are also observable and measurable values. Notice that the Miche criterion, which was conceived for plane waves, yields hardly acceptable values. Although the McCowan criterion was also conceived for plane waves, it considers "solitary waves" as individual waves in a train of finite waves and compares the surface pressures near the crest and the mean level. The third criterion, namely, the alternative velocity criterion, was a obtained using simulated considerations for our specific solution. However, it is clear that these results must be compared to in situ observations or experimental values.

Ultimately, it is important to emphasize the importance of the analytic approach to wind–wave interaction. In the past, deep or finite-depth coastlines were used for naval and commercial purposes. More recently, other human activities, such as recreation, habitat construction, tourism, or wind farms, have increased considerably. Therefore, predicting the evolution of waves near coasts is of practical importance.

Notice that the pure numerical modelling of this problem without recourse to theoretical developments has no chance of succeeding in the near or distant future because of the scale of energy dissipation, which is on the order of a micrometer, meaning that it would take 10^{25} mesh nodes to produce correct predictions on 100 km scales (Branger [45]). Therefore, the theoretical studies carried out in this research are essential.

Author Contributions: M.A.M. and A.L. have equally contributed to the present work. All authors have read and agreed to the published version of the manuscript.

Funding: This research received no external funding.

Conflicts of Interest: The authors declare no conflict of interest.

References

1. Li, T.; Shen, L. The principal stage in wind-wave generation. *J. Fluid Mech.* **2022**, *934*, A41.
2. Bonfils, A.; Mitra, D.; Moon, W.; Wettlaufer, J. Asymptotic interpretation of the Miles mechanism of wind-wave instability. *J. Fluid Mech.* **2022**, *944*, A8
3. Jeffreys, H. On the formation of water waves by wind. *Proc. R. Soc.* **1925**, *A107*, 189–206.
4. Jeffreys, H. On the formation of water waves by wind (Second paper). *Proc. R. Soc.* **1926**, *A110*, 241–247.
5. Phillips, O. On the generation of waves by turbulent wind. *J. Fluid Mech.* **1957**, *2*, 417–445.
6. Miles, J. Generation of surface waves by winds. *Appl. Mech. Rev.* **1997**, *50–57*, R5–R9.
7. Thomas, R.; Kharif, C.; Manna, M. A nonlinear Schrödinger equation for waves on finite depth with constant vorticity. *Phys. Fluids* **2012**, *24*, 138–149.
8. Montalvo, P.; Dorignac, J.; Manna, M.; Kharif, C.; Branger, H. Growth of surface wind-waves in water of finite depth. A theoretical approach. *Coast. Eng.* **2013**, *77*, 49–56.
9. Montalvo, P.; Kraenkel, R.; Manna, M.; Kharif, C. Wind-wave amplification mechanisms: Possible models for steep wave events in finite depth. *Nat. Hazards Earth Syst. Sci.* **2013**, *13*, 2805–2813.
10. Kadam, Y.; Patibandla, R.; Roy, A. Wind-generated waves on a water layer of finite depth. *J. Fluid Mech.* **2023**, *967*, A12.
11. Donelan, M.; Babanin, A.; Young, I.; Banner, M. Wave-Follower field measurements of the wind-input spectral function. Part II : Parameterization of the wind input. *J. Phys. Oceanogr.* **2006**, *36*, 1672–1689.
12. Donelan, M.; Skafel, M.; Graber, H.; Liu, P.; Schwab, D.; Venkatesh, S. On the growth rate of wind-generating waves. *Atmos.-Ocean.* **1992**, *30*, 457–478.
13. Young, I. The growth rate of finite depth wind-generated waves. *Coast. Eng.* **1997**, *32*, 181–195.
14. Young, I. *Wind Generated Ocean Waves*; Elsevier Science: Amsterdam, The Netherlands, 1999.
15. Branger, H.; Manna, M.; Luneau, C.; Abid, M.; Kharif, C. Growth of surface wind-waves in water of finite depth: A laboratory experiment. *Coast. Eng.* **2022**, *177*, 104174. https://doi.org/10.1016/j.coastaleng.2022.104174.
16. Whitham, G. *Linear and Nonlinear Waves*; Wiley: New York, NY, USA, 1974.
17. Benney, D.J. Long waves in liquid films. *J. Math. Phys.* **1996**, *45*, 150–155.
18. Johnson, R. Shallow water waves on a viscous fluid-the undular bore. *Phys. Fluids* **1972**, *15*, 1693–1699.

19. Grad, H.; Hu, P. Unified shock in plasma. *Phys. Fluids* **1967**, *10*, 2596–2602.
20. Hu, P. Collisional theory of shock and nonlinear waves in plasma. *Phys. Fluids* **1972**, *15*, 854–864.
21. Wadati, M. Wave propagation in nonlinear lattice. *J. Phys. Soc. Jpn.* **1975**, *38*, 673–680.
22. Karahara, T. Weak nonlinear magneto-acoustic waves in a cold plasma in the presence of effective electron-ion collisions. *J. Phys. Soc. Jpn.* **1970**, *27*, 1321–1329.
23. Serre, F. Contribution à L'étude des écoulements Permanents et Variables Dans Les Canaux. *La Houille Blanche* **1953**, *3*, 830–872.
24. Green, A.; Laws, N.; Naghdi, P.M. On the theory of water waves. *Proc. R. Soc. A* **1974**, *338*, 48–35.
25. Green, A.; Naghdi, P.M. A Derivation of Equations for Wave Propagation in Water of Variable Depth. *Fluid. Mech.* **1976**, *78*, 237–246.
26. Su, C.; Gardner, C. Collisional theory of shock and nonlinear waves in plasma. *J. Math. Phys.* **1969**, *10*, 536–539.
27. Shah, N.A.; Alyousef, H.A.; El-Tantawy, S.A.; Shah, R.; Chung, J.D. Analytical Investigation of Fractional-Order Korteweg–De-Vries-Type Equations under Atangana–Baleanu–Caputo Operator: Modeling Nonlinear Waves in a Plasma and Fluid. *Symmetry* **2022**, *14*, 739. https://doi.org/10.3390/sym14040739.
28. Shah, N.A.; Agarwal, P.; Chung, J.D.; El-Zahar, E.R.; Hamed, Y.S. Analysis of Optical Solitons for Nonlinear Schrödinger Equation with Detuning Term by Iterative Transform Method. *Symmetry* **2020**, *12*, 1850. https://doi.org/10.3390/sym12111850.
29. Zhang, R.; Shakeel, M.; Turki, N.B.; Shah, N.A.; Tag, S.M. Novel analytical technique for mathematical model representing communication signals: A new travelling wave solutions. *Results Phys.* **2023**, *51*, 106576.
30. Shakeel, M.; Manan, A.; Bin Turki, N.; Shah, N.; Tag, S. Novel analytical technique to find diversity of solitary wave solutions for Wazwaz-Benjamin-Bona Mahony equations of fractional order. *Results Phys.* **2023**, *51*, 106671.
31. Manna, M.A.; Latifi, A.; Kraenkel, R.A. Green–Naghdi dynamics of surface wind waves in finite depth. *Fluid Dyn. Res.* **2018**, *50*, 025514. https://doi.org/10.1088/1873-7005/aaa739.
32. Adriani, O.; Barbarino, G.; Bazilevskaya, G.; Bellotti, R.; Boezio, M.; Bogomolov, E.; Bonechi, L.; Bongi, M.; Bonvicini, V.; Bottai, S.; et al. An anomalous positron abundance in cosmic rays with energies 1.5–100 GeV. *Nature* **2009**, *458*, 607–609. https://doi.org/10.1038/nature07942.
33. Cheng, S.; Liu, H. On adjustable undular bore profiles based on the modified steady KdV–Burgers equation. *J. Hydraul. Res.* **2023**, *61*, 322–332 .
34. Manna, M.A.; Montalvo, P.; Kraenkel, R.A. Finite time blow-up and breaking of solitary waves. *Phys. Rev. E* **2014**, *90*, 013006.
35. Dunkel, O. Some applications of Green's theorem in one dimension. *Bull. Am. Math. Soc.* **1902**, *8*, 288–292.
36. Svendsen, I.A. *Introduction to Nearshore Hydrodynamics*; World Scientific: Londin, UK, 2005. https://doi.org/10.1142/5740.
37. Chiang, C.M. *The Applied Dynamics of Ocean Surface Waves*; World Scientific: Londin, UK, 1992. https://doi.org/10.1142/0752.
38. Ott, E.; Sudan, R.N. Damping of Solitary Waves. *Phys. Fluids* **1970**, *13*, 1432–1434. https://doi.org/10.1063/1.1693097.
39. Ott, E.; Sudan, R.N. Nonlinear Theory of Ion Acoustic Waves with Landau Damping. *Phys. Fluids* **1969**, *12*, 2388–2394. https://doi.org/10.1063/1.1692358.
40. Manna, M.; Latifi, A. Serre-Green-Naghdi Dynamics under the Action of the Jeffreys' Wind-Wave Interaction. *Fluids* **2022**, *7*, 266. https://doi.org/10.3390/fluids7080266.
41. Darboux, G. *Leçons sur la Théorie Générale des Surfaces*; CreateSpace: Scotts Valley, CA, USA, 2016.
42. McCowan, J. On the highest wave of permanent type. *Philos. Mag. Ser. 5* **1894**, *38*, 351–358.
43. Miche, R. *Mouvement Ondulatoires de la Mer en Profondeur Constante ou Décroissante*; École Nationale des Ponts et Chaussées: Marne-la-Vallée, France, 1944.
44. Shemer, L. On kinematics of very steep waves. *Nat. Hazards Earth Syst. Sci.* **2013**, *13*, 2101–2107.
45. Branger, H. (CNRS, Marseille, France). Personal communication. 2021.